Stabilization of superoxidized form of synthetic Fe_4S_4 cluster as the first model of high potential iron sulfur proteins in aqueous media

Hide Kambayashi, Hirotaka Nagao and Koji Tanaka*
Department of Structural Molecular Science, The Graduate University for Advanced Studies, Institute for Molecular Science, Myodaiji, Okazaki 444 (Japan)

Masami Nakamoto
Osaka Municipal Technical Research Institute, Morinomiya, Joto-ku, Osaka 565 (Japan)

Shie-Ming Peng
Department of Chemistry, National Taiwan University, Roosevelt Road Section 4, Taipei, Taiwan 10764 (ROC)

(Received January 11, 1993; revised March 17, 1993)

Abstract

The adamantanethiolate ligated Fe_4S_4 cluster, $[Fe_4S_4(SAd)_4]^{2-}$, exhibits two stable $[Fe_4S_4]^{2+/+}$ and $[Fe_4S_4]^{3+/2+}$ redox couples in dry DMF, while $[Fe_4S_4(SAd)_4]^-$ readily undergoes a hydrolysis reaction by the addition of a small amount of H_2O in DMF (3 vol.%). The hydrolysis of $[Fe_4S_4(SAd)_4]^-$ can be effectively depressed by the presence of free AdSH in H_2O/DMF, and also by solubilization in aqueous PDAH solutions (PDAH = poly[2-(dimethylamino)hexanamide]). The observation that the crystal structure of $(Ph_4As)_2[Fe_4S_4(SAd)_4]$ has enough space for coordination of H_2O to the Fe_4S_4 core indicates that stabilization of $[Fe_4S_4(SAd)_4]^-$ in aqueous media is ascribed to depression of dissociation of AdS^- from the $[Fe_4S_4]^{3+}$ core rather than hydrophobic spheres around the $[Fe_4S_4]^{3+}$ core.

Introduction

4 Fe-iron sulfur proteins operate among three different oxidation states, $[Fe_4S_4]^+$, $[Fe_4S_4]^{2+}$ and $[Fe_4S_4]^{3+}$ (Scheme 1) [1, 2].

$$\underset{Fd_{red}}{[Fe_4S_4]^+} \rightleftharpoons \underset{Fd_{ox},\ Hp_{red}}{[Fe_4S_4]^{2+}} \rightleftharpoons \underset{Hp_{ox}}{[Fe_4S_4]^{3+}}$$

Scheme 1.

Ferredoxins (Fd) exhibit the $[Fe_4S_4]^{2+/+}$ redox couple around −0.7 V versus SCE, while high potential iron sulfur proteins (Hp) show the $[Fe_4S_4]^{3+/2+}$ couple around 0 V at pH 7 [3, 4]. Although there is no clear difference in the structures of the Fe_4S_4 cores between Hp and Fd [2], oxidation of the $[Fe_4S_4]^{2+}$ core of *Azotobacter vinelandii* Ferredoxin I leads to the loss of one of the Fe atoms and a 3Fe cluster is formed [5]. X-ray structural data of *Chromatium vinosum* Hp suggests that the Fe_4S_4 core is buried in hydrophobic protein environments [6]. Stability of the $[Fe_4S_4]^{3+}$ state (Hp_{ox}), therefore, has been explained in terms of protection of the Fe_4S_4 core from water attack by hydrophobic protein environments around Fe_4S_4 cores [5].

Synthetic Fe_4S_4 clusters, $[Fe_4S_4(SR)_4]^{2-}$ (R = alkyl or aryl), usually display a reversible or pseudo-reversible $[Fe_4S_4(SR)_4]^{2-/3-}$ redox couple in organic or aqueous solutions, and some of them also show the $[Fe_4S_4(SR)_4]^{-/2-}$ redox couple in less polar organic solvents such as CH_2Cl_2, $C_6H_5NO_2$ and C_6H_5CN [7]. Most synthetic Fe_4S_4 clusters, however, decompose upon oxidation in polar solvents such as CH_3CN and DMF**. The superoxidized form, $[Fe_4S_4(SR)_4]^-$, therefore, is considered to be much more unstable than the oxidized and reduced forms ($[Fe_4S_4(SR)_4]^{n-}$ ($n = 2, 3$)) in polar solvents. In fact, sterically encumbered ligands such as t-butylthiolate [8], 2,4,6-tri(i-propyl)benzenethiolate [9, 10], polypeptide [9], and the 36-membered ring [11] have been shown to stabilize the superoxidized form in polar organic solvents by protection of the $[Fe_4S_4]^{3+}$ core from solvent attack, and the structure of $[Fe_4S_4(SC_6H_2(i\text{-}C_3H_7)_3)_4]^-$ is determined by X-ray

*Author to whom correspondence should be addressed.

**For example, a cyclic voltammogram of $[Fe_4S_4(SPh)_4]^{2-}$ in CH_2Cl_2 shows a pseudo-reversible (2−/−) couple at $E_{1/2} = -0.32$ V versus SCE, while $[Fe_4S_4(SPh)_4]^{2-}$ undergoes an irreversible oxidation around 0 V in polar solvents such as CH_3CN and DMF.

0020-1693/93/$6.00

analysis [10]. The redox behaviour of the $[Fe_4S_4(SR)_4]^{-/2-}$ couple in aqueous media, therefore, is of particular interest since the stability of the $[Fe_4S_4]^{3+}$ core of the synthetic Fe_4S_4 clusters has not been studied in aqueous media. This paper describes the redox behaviour of $[Fe_4S_4(SAd)_4]^{2-}$ (Ad = adamantane) as the first example of an Hp model in aqueous conditions. Part of this work has been reported elsewhere [12].

Experimental

General

Tetraethylammonium and tetraphenylarsonium salts of $[Fe_4S_4(SAd)_4]^{2-}$ (Ad = adamantane) were prepared according to a literature method [12]. Single crystals of $(Ph_4As)_2[Fe_4S_4(SAd)_4]$ were obtained by recrystallization from CH_3CN. *N,N*-Dimethylformamide (DMF) was purified by distillation over CaH_2 under reduced pressure and stored under N_2. All manipulations were carried out under an N_2 atmosphere. Poly[2-(dimethylamino)hexanamide] (PDAH) kindly supplied by Toray Co., Ltd. was purified by dialysis.

Solubilization of $(Et_4N)_2[Fe_4S_4(SAd)_4]$ in aqueous PDAH solutions

A DMF solution (1.0 cm^3) of $(Et_4N)_2[Fe_4S_4(SAd)_4]$ (1.3 μmol) was added to a stirred aqueous solution of PDAH (0.1 g) (25 cm^3, pH 6–10.5 adjusted with 0.1 M aqueous H_3PO_4 and NaOH solutions), and the solution was then sonicated with a 120 W New Bransonic B3200 J3 under N_2 for 5 s.

Physical measurements

Electronic absorption spectra were measured with a Hewlett-Packard 8452A spectrophotometer. Cyclic voltammetry was performed using a Hokuto Denko HA-501 potentiostat/galvanostat with a glassy carbon disk or indium trioxide coated glass (ITO), Pt plate, and saturated calomel electrode (SCE)* as the working, auxiliary, and reference electrodes, respectively. 0.1 M Tetraethylammonium perchlorate and 0.1 M NaOH–H_3PO_4 were used as the supporting electrolytes in DMF and water, respectively, and the concentration of $(Et_4N)_2[Fe_4S_4(SAd)_4]$ was adjusted to *c.* 1×10^{-3} M. Spectroelectrochemical experiments were carried out using an optically transparent thin-layer electrode consisting of a Pt-gauze electrode in a 0.5 mm width quartz cuvette, a Pt-wire auxiliary electrode, and an SCE [13]. An aqueous PDAH solution of $(Et_4N)_2[Fe_4S_4(SAd)_4]$ was titrated with 0.05 M aqueous H_2SO_4 solution using a Hiranuma Reporting Titrator (comitite-8).

*$E(Fc^{0/+}) = E(SCE) + 0.39$ V; $E(SHE) = E(SCE) + 0.242$ V.

X-ray crystallographic studies

The reflections from X-ray analyses were collected by θ–2θ techniques ($0 < 2\theta < 50°$) on an Enraf-Nonius CAD4 automated four-circle diffractometer with Mo Kα radiation (0.70930 Å). The 4484 independent reflections with $F_o > 2\sigma(F_o)$ were used for the structure refinement. All the calculations were carried out on a VAX 3800 computer, using the NRCC-SDP program. The structures were solved by the direct method. Non-hydrogen atoms were refined anisotropically, and hydrogen atoms were refined isotropically.

Results and discussion

Redox behaviour of $[Fe_4S_4(SAd)_4]^{2-}$ in DMF and aqueous media

The cyclic voltammogram (CV) of $(Et_4N)_2[Fe_4S_4(SAd)_4]$** using a glassy carbon disk electrode exhibits not only the $[Fe_4S_4(SAd)_4]^{2-/3-}$ redox couple ($E_{pc} = -1.36$; $E_{pa} = -1.28$ V versus SCE) but also the $[Fe_4S_4(SAd)_4]^{-/2-}$ one ($E_{pa} = -0.06$; $E_{pc} = -0.14$ V) in DMF (Fig. 1(a)). The $E_{1/2}$ ($E_{1/2} = (E_{pc} + E_{pa})/2$) values of -1.32 and -0.10 V are close to those of the $[Fe_4S_4(S\text{-}t\text{-}Bu)_4]^{2-/3-}$ and $[Fe_4S_4(S\text{-}t\text{-}Bu)_4]^{-/2-}$ couples ($E_{1/2} = -1.42$ and -0.12 V) in DMF [8]. The stability of both $[Fe_4S_4(SAd)_4]^{3-}$ and $[Fe_4S_4(SAd)_4]^{-}$ in the redox cycle in DMF was also observed in the electronic absorption spectra; $(Et_4N)_2[Fe_4S_4(SAd)_4]$ in DMF shows two absorption bands at 418 and 318 nm (Fig. 2). Those bands shifted to 380 and 300 nm when $[Fe_4S_4(SAd)_4]^{2-}$ was reduced to $[Fe_4S_4(SAd)_4]^{3-}$ at -1.40 V. The reoxidation of the resulting solution at -1.10 V regenerated the original

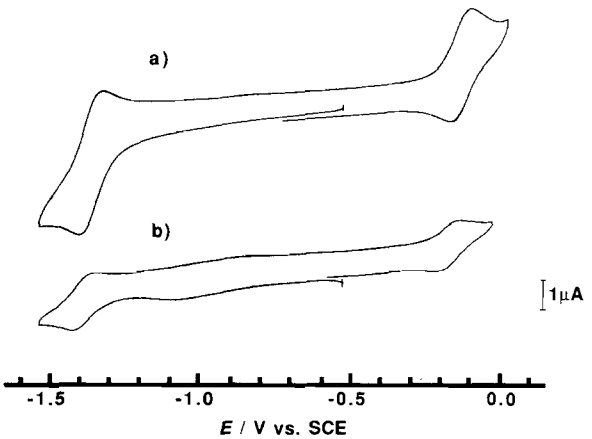

Fig. 1. Cyclic voltammograms of $(Et_4N)_2[Fe_4S_4(SAd)_4]$ (1×10^{-3} mol/dm^3) in dry DMF (a) and in the presence of AdSH (3×10^{-2} mol/dm^3) in H_2O/DMF (23 vol.%) (b); $dE/dt = 0.1$ V/s.

**$(Ph_4As)_2[Fe_4S_4(SAd)_4]$ is not suitable for cyclic voltammetry, since Ph_4As^+ undergoes an irreversible reduction at potentials more negative than -1.4 V.

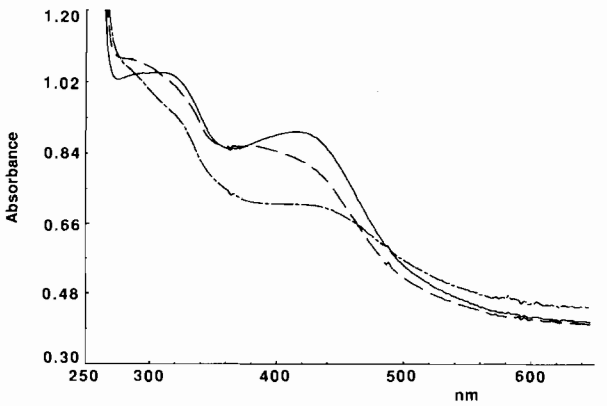

Fig. 2. Electronic absorption spectra of $[Fe_4S_4(SAd)_4]^{2-}$ (——), $[Fe_4S_4(SAd)_4]^{3-}$ (– – –), and $[Fe_4S_4(SAd)_4]^{-}$ (— – —) in DMF; the latter two were prepared under the controlled potential electrolysis of $(Et_4N)_2[Fe_4S_4(SAd)_4]$ at −1.40 and 0.10 V vs. SCE in DMF.

absorption spectrum of $[Fe_4S_4(SAd)_4]^{2-}$. The electrochemical oxidation from $[Fe_4S_4(SAd)_4]^{2-}$ to $[Fe_4S_4(SAd)_4]^{-}$ at 0.10 V in the same solvent resulted in a red shift of the 418 and 318 nm bands of $[Fe_4S_4(SAd)_4]^{2-}$ to 430 and 326 nm, and the electrochemical reduction of the solution at −1.10 V recovered the 418 and 318 nm bands. The absorptivities of the 418 and 318 nm bands regenerated in the reduction for 30 min were almost identical to those of the original bands of $[Fe_4S_4(SAd)_4]^{2-}$.

The $[Fe_4S_4(SAd)_4]^{-/2-}$ redox couple in DMF is more significantly influenced by the presence of H_2O than the $[Fe_4S_4(SAd)_4]^{2-/3-}$ one. The CV of $[Fe_4S_4(SAd)_4]^{2-}$ in the presence of a small amount of H_2O (3 vol.%) showed a strong irreversible oxidation current at a potential more positive than 0.1 V, and the cathodic wave at −0.14 V of the $[Fe_4S_4(SAd)_4]^{-/2-}$ couple completely disappeared. On the other hand, the cathodic and anodic waves of the reversible $[Fe_4S_4(SAd)_4]^{2-/3-}$ couple were observed at the same potentials as those in dry DMF. This result clearly indicates that $[Fe_4S_4(SAd)_4]^{-}$ is much more prone to hydrolysis than $[Fe_4S_4(SAd)_4]^{2-}$ and $[Fe_4S_4(SAd)_4]^{3-}$ in H_2O/DMF. It is well known that the water soluble clusters, $[Fe_4S_4L_4]^{2-}$ (L = SCH_2CH_2OH or Cys(Ac)NHMe), are subject to hydrolysis in water [14]. The redox potentials of the $[Fe_4S_4L_4]^{2-/3-}$ couples in aqueous conditions, therefore, have been determined in the presence of excess ligands [14]. In accord with this, the CV of $(Et_4N)_2[Fe_4S_4(SAd)_4]$ shows both the $[Fe_4S_4(SAd)_4]^{2-/3-}$ and $[Fe_4S_4(SAd)_4]^{-/2-}$ couples in the presence of a 30 molar amount of free AdSH even in H_2O/DMF (23 vol.%) (Fig. 1(b)). The distinct difference in the stability of $[Fe_4S_4(SAd)_4]^{-}$ in the absence and presence of free AdSH is reasonably explained by depression of dissociation of the AdS^{-} ligand from the $[Fe_4S_4]^{3+}$ core in H_2O/DMF. This view also implies that the affinity of H_2O to the $[Fe_4S_4]^{3+}$ core is much stronger than that to the $[Fe_4S_4]^{2+}$ and $[Fe_4S_4]^{+}$ ones.

We have shown that hydrolysis of $[Fe_4S_4(SR)_4]^{2-}$ (R = alkyl or aryl) can be effectively inhibited in aqueous micellar solutions [15]. Poly[2-(dimethylamino)-hexamide] (PDAH), know as water soluble nylon, in place of the usual surface active agents was used to solubilize $(Et_4N)_2[Fe_4S_4(SAd)_4]$ in H_2O. In aqueous conditions, surface active agents often cause one serious disadvantage in electrochemical measurements because of adsorption on the surface of an electrode, and strongly interfere with the direct electron transfer between the electroactive species and the electrode [15]. In fact, a glassy carbon electrode gave very broad redox waves in the CV of $(Et_4N)_2[Fe_4S_4(SAd)_4]$ solubilized in an aqueous PDAH solution presumably due to adsorption of PDAH on the electrode. On the other hand, an ITO disk electrode clearly shows the redox couples of not only $[Fe_4S_4(SAd)_4]^{2-/3-}$ ($E_{1/2} = -0.88$ V) but also $[Fe_4S_4(SAd)_4]^{-/2-}$ ($E_{1/2} = -0.28$ V) at pH 7.3 (Fig. 3(a)). A disagreement over the areas between the cathodic and anodic waves of the $[Fe_4S_4(SAd)_4]^{2-/3-}$ couple may be associated with the stronger adsorption of $[Fe_4S_4(SAd)_4]^{2-}$ than $[Fe_4S_4(SAd)_4]^{3-}$ on the ITO electrode. The current intensities of the cathodic and anodic waves of the $[Fe_4S_4(SAd)_4]^{2-/3-}$ and $[Fe_4S_4(SAd)_4]^{-/2-}$ couples are dependent on the pH of the aqueous phase due to competitive adsorption among the PDAH, (3−), (2−) and (1−) state of the clusters at different pHs (Fig. 3(b)). It should be noticed that both the $[Fe_4S_4(SAd)_4]^{2-/3-}$ and $[Fe_4S_4(SAd)_4]^{-/2-}$ redox couples are clearly observed even in the absence of free AdSH in the aqueous PDAH solutions. Thus, PDAH effectively protects against hydrolysis of $[Fe_4S_4(SAd)_4]^{-}$ in H_2O. As can be seen in Fig. 3(a) and (b), the cathodic and anodic peak potentials of both the $[Fe_4S_4(SAd)_4]^{2-/3-}$ and $[Fe_4S_4(SAd)_4]^{-/2}$

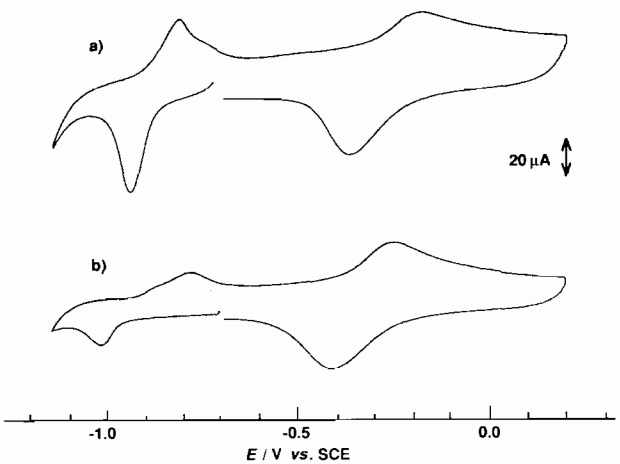

Fig. 3. Cyclic voltammograms of $(Et_4N)_2[Fe_4S_4(SAd)_4]$ in aqueous PDAH solution at pH 7.3 (a) and 8.0 (b); $dE/dt = 0.1$ V/s.

couples are shifted with changes in the pH of the aqueous PDAH solutions. Figure 4 shows the $E_{1/2}^{red}$ values of the $[Fe_4S_4(SAd)_4]^{2-/3-}$ couple ($E_{1/2}^{red} = (E_{pc} + E_{pa})/2$) and $E_{1/2}^{ox}$ values of the $[Fe_4S_4(SAd)_4]^{-/2-}$ one ($E_{1/2}^{ox} = (E_{pc} + E_{pa})/2$) at various pHs in an aqueous PDAH solution. The $E_{1/2}^{red}$ value is shifted by -0.065 V/pH in the pH range of *c.* 6.5 to 9.4, and has a tendency to level off beyond the pH region (● in Fig. 4). On the basis of the fact that $[Fe_4S_4(SR)_4]^{n-}$ (R = alkyl or aryl; $n = 2, 3$) undergoes a reversible protonation of core and/or terminal sulfur atoms in aqueous micellar solutions [15], the shift of -0.065 V/pH of $E_{1/2}^{red}$ is rationalized in terms of participation of one proton in the redox reaction of the $[Fe_4S_4(SAd)_4]^{2-/3-}$ couple in these pH ranges. The $E_{1/2}^{ox}$ value of the $[Fe_4S_4(SAd)_4]^{-/2-}$ couple is also shifted by -0.075 V/pH in the pH range of 10 to 7 with a flat region around pH 7.0 (○ in Fig. 4). Although the shift of the $E_{1/2}^{ox}$ value (-0.075 V/pH) is somewhat larger than the theoretical value of the H^+/e^- transfer (-0.063 V/pH), one proton is considered to participate in the $[Fe_4S_4(SAd)_4]^{-/2-}$ redox reaction in the aqueous PDAH solution from analogy with the $[Fe_4S_4(SAd)_4]^{2-/3-}$ redox couple. The flat region of $E_{1/2}^{ox}$ around pH 7, therefore, indicates that the proton does not participate in the $[Fe_4S_4(SAd)_4]^{-/2-}$ redox reaction.

pH titration of $(Et_4N)_2[Fe_4S_4(SAd)_4]$ in aqueous PDAH solutions

The protonation behaviour of $[Fe_4S_4(SAd)_4]^{2-}$ was also examined by means of pH titration in aqueous PDAH solutions, because the shift of -0.065 V/pH of the $E_{1/2}$ values merely implies participation of one proton in the redox reactions of the $[Fe_4S_4(SAd)_4]^{2-/3-}$ and $[Fe_4S_4(SAd)_4]^{-/2-}$ couples. The aqueous PDAH solutions were titrated in the absence and presence of $(Et_4N)_2[Fe_4S_4(SAd)_4]$ using 0.05 M H_2SO_4* in order to remove the effect resulting from reversible protonation of PDAH. The addition of a DMF solution (1.0 cm^3) of $(Et_4N)_2[Fe_4S_4(SAd)_4]$ (6.4 μmol) to an aqueous PDAH solution (25 cm^3) of pH 9.75 (adjusted with 0.1N aqueous NaOH) resulted in a shift of the solution to pH 10.65. This result indicates that protonation of $[Fe_4S_4(SAd)_4]^{2-}$ takes place above pH 9.7. Titration, therefore, was started from pH 10.5 of the aqueous phase. Reproducible titration data were obtained between pH 6 and 10.5, and an irreversible protonation of $[Fe_4S_4(SAd)_4]^{2-}$ occurred at pHs below 5.5. Figure 5 shows the titration curves in the absence (□) and presence of $(Et_4N)_2[Fe_4S_4(SAd)_4]$ (△), and the difference in the amount of H_2SO_4 consumed in both titrations (○). The inset of Fig. 5 represents the number of protons consumed for the protonation of $[Fe_4S_4(SAd)_4]^{2-}$ calculated from the titration curve (solid line) at each pH. In the pH region below 8, most of the protons are consumed by protonation of PDAH (□ and △ in Fig. 5). However, PDAH does not seriously interfere in the pH titration of $[Fe_4S_4(SAd)_4]^{2-}$ in the pH region above 8, and the calculated curve clearly indicates that $[Fe_4S_4(SAd)_4]^{2-}$ exists as the mono-protonated form, $[Fe_4S_4$-

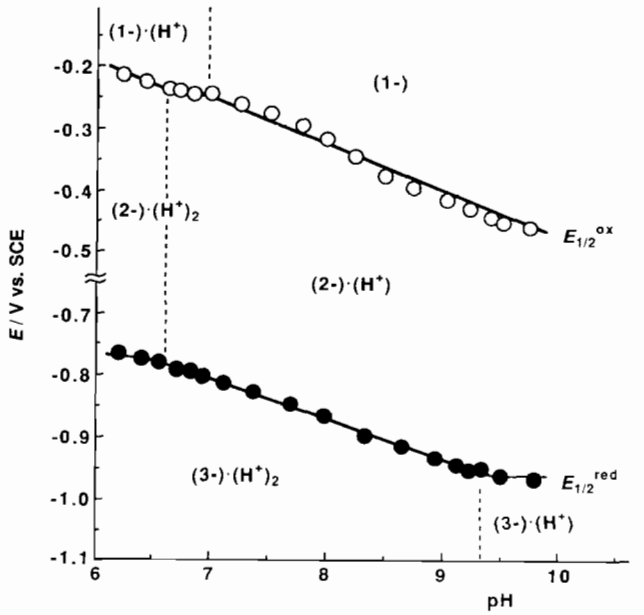

Fig. 4. $E_{1/2}^{ox}$ and $E_{1/2}^{red}$ values of the $[Fe_4S_4(SAd)_4]^{2-/-}$ and $[Fe_4S_4(SAd)_4]^{2-/3-}$ couples at various pH in aqueous PDAH solutions.

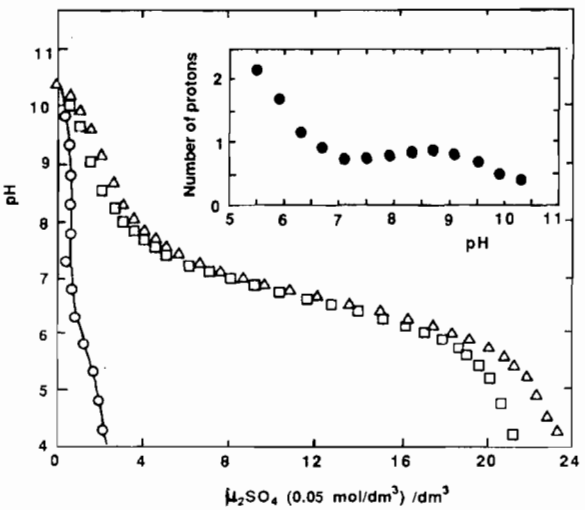

Fig. 5. Titration of aqueous PDAH solutions in the absence (□) and presence of $(Et_4N)_2[Fe_4S_4(SAd)_4]$ (△), and the difference in two curves (○). Inset: amount of protons consumed in protonation of $(Et_4N)_2[Fe_4S_4(SAd)_4]$.

*pH titration of the aqueous PDAH solution of $(Et_4N)_2[Fe_4S_4(SAd)_4]$ was started from pH around 10.5 using 0.05 M of an aqueous H_2SO_4 solution due to the acid lability of the cluster, and the aqueous PDAH solution (25 cm^3) containing 1.0 cm^3 of DMF was titrated as a blank test.

$(SAd)_4]^{2-}\cdot(H^+)$, below pH 9 (inset of Fig. 5). Furthermore, the curve in the inset also suggests the occurrence of the successive protonation of $[Fe_4S_4(SAd)_4]^{2-}\cdot(H^+)$ below pH 7, although the value in that pH region involves somewhat uncertainty in the absolute accuracy due to the protonation of PDAH. Therefore, the first and second protonation of $[Fe_4S_4(SAd)_4]^{2-}$ may begin to take place around pH 10 and 7 in the aqueous PDAH solution (eqns. (1) and (2)).

$$[Fe_4S_4(SAd)_4]^{2-} + H^+ \rightleftharpoons [Fe_4S_4(SAd)_4]^{2-}\cdot(H^+) \quad (1)$$

$$[Fe_4S_4(SAd)_4]^{2-}\cdot(H^+) + H^+ \rightleftharpoons [Fe_4S_4(SAd)_4]^{2-}\cdot(H^+)_2 \quad (2)$$

Protonation behaviour of $[Fe_4S_4(SAd)_4]^{3-}$ in the PDAH solution can be deduced from the results of the pH titration of $[Fe_4S_4(SAd)_4]^{2-}$ (eqns. (1) and (2)) and the $E_{1/2}^{red}$ value of the $[Fe_4S_4(SAd)_4]^{2-/3-}$ couple (Fig. 4) in the aqueous PDAH solution. Independence of the $E_{1/2}^{red}$ value of pH above 9.4 may be explained by the presence of mono-protonated $[Fe_4S_4(SAd)_4]^{3-}$ as similar to $[Fe_4S_4(SAd)_4]^{2-}\cdot(H^+)$ (eqn. (1)). The second protonation of $[Fe_4S_4(SAd)_4]^{3-}\cdot(H^+)$ would cause the shift by -0.065 V/pH of $E_{1/2}^{red}$ in the pH region of 9.4 to 6.5, and the flat region of $E_{1/2}^{red}$ below 6.5 is interpreted as the existence of both $[Fe_4S_4(SAd)_4]^{2-}\cdot(H^+)_2$ and $[Fe_4S_4(SAd)_4]^{3-}\cdot(H^+)_2$. Similarly, protonation of $[Fe_4S_4(SAd)_4]^-$ is inferred from the $E_{1/2}^{ox}$ value of the $[Fe_4S_4(SAd)_4]^{-/2-}$ couple (Fig. 4). The existence of a flat region of $E_{1/2}^{ox}$ around pH 7.0 strongly suggests the presence of the mono-protonated form of $[Fe_4S_4(SAd)_4]^-$, because the shift of $E_{1/2}^{ox}$ below pH 6.5 (Fig. 4) is explained by the second protonation of $[Fe_4S_4(SAd)_4]^{2-}\cdot(H^+)$ (eqn. (2)).

The redox potential of the $[Fe_4S_4(SR)_4]^{2-/3-}$ (R = alkyl or aryl) couple in aqueous solutions has been shown to shift to positive potentials compared with that in organic solvents [14, 15]. In accord with this, $E_{1/2}^{red}$ of the present Fe_4S_4 cluster is observed at more positive potentials (0.25–0.70 V) in aqueous PDAH solution than that in DMF. On the other hand, $E_{1/2}^{ox}$ shifts to negative potentials in aqueous solutions even at pH 6.0, where $E_{1/2}^{ox}$ shows the most positive value in the experimental pH range. There has been no report concerning the redox behaviour of the $[Fe_4S_4(SR)_4]^{-/2-}$ (R = alkyl or aryl) couple in aqueous conditions so far. The positive shifts of both $E_{1/2}^{red}$ and $E_{1/2}^{ox}$ values with decreasing pH are reasonably explained by the protonation of not only $[Fe_4S_4(SAd)_4]^{2-/3-}$, but also $[Fe_4S_4(SAd)_4]^-$. The reverse shift of $E_{1/2}^{red}$ and $E_{1/2}^{ox}$ between DMF and aqueous solutions, however, is not clear in the present study.

Crystal structure of $(Ph_4As)_2[Fe_4(SAd)_4]$

X-ray analysis of a single crystal of $(Ph_4As)_2[Fe_4S_4(SAd)_4]$ was conducted to elucidate the hydrophobic spheres around the Fe_4S_4 core*. The molecular structure of $(Ph_4As)_2[Fe_4S_4(SAd)_4]$ is depicted in Fig. 6. The data for crystal structure analysis are tabulated in Table 1, and the selected bond lengths and angles of $(Ph_4As)_2[Fe_4S_4(SAd)_4]$ together with those of $(Me_3NCH_2Ph)_2[Fe_4S_4(S\text{-}t\text{-}Bu)_4]$ [8] for comparison are shown in Table 2. Each iron is tetrahedrally coordinated by three core sulfurs (S*) and one terminal sulfur (S) of the AdS^- ligand. The Fe_4S_4 core is approximated by D_{2d} symmetry, similar to the structure of $[Fe_4S_4(S\text{-}t\text{-}Bu)_4]^{2-}$ [3]. The 12 Fe–S* bonds are divided into two groups: 4 short Fe–S* bonds (2.237(3)–2.268(3) Å) parallel to the S_4 axis and 8 long Fe–S* bonds (2.298(3)–2.331(3) Å) perpendicular to the S_4 axis. The mean values of bond length of the 4 short Fe–S* and 8 long Fe–S* bonds are 2.252(16) and 2.315(10) Å, respectively, which are essentially consistent with those of $[Fe_4S_4(S\text{-}t\text{-}Bu)_4]^{2-}$ (Table 2). It is

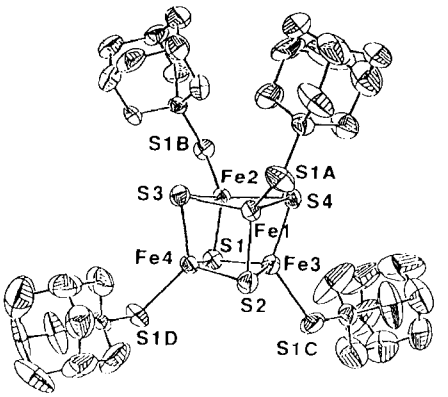

Fig. 6. Molecular structure of $[Fe_4S_4(SAd)_4]^{2-}$.

TABLE 1. Crystallographic data for $(Ph_4As)_2[Fe_4S_4(SAd)_4]$

Formula	$C_{88}H_{100}S_8As_2Fe_4$
Formula weight	1787.47
Crystal system	orthorhombic
Space group	$P2_12_12_1$
a (Å)	14.176(4)
b (Å)	22.059(7)
c (Å)	26.515(5)
V (Å^3)	8291(4)
Z	4
ρ_{calc} (g cm^{-3})	1.432
Radiation	Mo Kα (λ = 0.70930 Å)
Absorption coefficient, μ (cm^{-1})	17.1
R	0.044
R_w	0.041

*Since suitable crystals of $(Et_4N)_2[Fe_4S_4(SAd)_4]$ were not obtained, single crystals of $(Ph_4As)_2[Fe_4S_4(SAd)_4]$ were used for the X-ray analysis.

TABLE 2. Selected distances (Å) and angles (°) in $[Fe_4S_4(SAd)_4]^{2-}$ and comparison with data in $[Fe_4S_4(S\text{-}t\text{-}Bu)_4]^{2-}$ [8]

	AdS^-	$t\text{-}BuS^-$		AdS^-	$t\text{-}BuS^-$
	Fe---Fe			Fe–S*	
Fe(1)–Fe(2)	2.7517(24)	2.745(2)	Fe(1)–S(2)	2.237(3)	2.242(3)
Fe(3)–Fe(4)	2.7010(22)	2.723(2)	Fe(2)–S(1)	2.238(3)	2.250(2)
Mean	2.7264(36)	2.734	Fe(3)–S(4)	2.264(3)	2.260(3)
			Fe(4)–S(3)	2.268(3)	2.255(2)
Fe(1)–Fe(3)	2.7511(22)	2.755(2)	Mean	2.252(16)	2.252(8)
Fe(1)–Fe(4)	2.7840(22)	2.753(2)			
Fe(2)–Fe(3)	2.8130(22)	2.773(2)	Fe(1)–S(3)	2.320(3)	2.308(2)
Fe(2)–Fe(4)	2.7563(20)	2.766(2)	Fe(1)–S(4)	2.318(3)	2.316(3)
Mean	2.7761(28)	2.767(10)	Fe(2)–S(3)	2.320(3)	2.323(3)
Mean (of 6)	2.7595(37)	2.756(20)	Fe(2)–S(4)	2.331(3)	2.315(2)
			Mean	2.322(6)	2.316(6)
	Fe–S				
Fe(1)–S(1A)	2.270(4)	2.258(3)	Fe(3)–S(1)	2.307(3)	2.318(3)
Fe(2)–S(1B)	2.273(3)	2.269(3)	Fe(3)–S(2)	2.316(3)	2.312(3)
Fe(3)–S(1C)	2.266(3)	2.259(2)	Fe(4)–S(1)	2.311(3)	2.319(3)
Fe(4)–S(1D)	2.259(3)	2.258(3)	Fe(4)–S(2)	2.298(3)	2.309(3)
Mean	2.267(6)	2.261(5)	Mean	2.308(7)	2.315(5)
			Mean (of last 8)	2.315(10)	2.315(5)

worth noting that the Fe–S* bonds in the face formed by Fe(1)S*(3)Fe(2)S*(4) atoms (mean 2.322(6) Å) are slightly longer than those in Fe(3)S*(1)Fe(4)S*(2) (mean 2.308(7) Å). The distance between Fe(1) and Fe(2) (2.7517(24) Å) is also longer than that of Fe(3) and Fe(4) (2.7010(22) Å). A similar distortion has been reported in the crystal structure of $(Et_4N)_2[Fe_4S_4(SCH_2C_6H_5)_4]$, but the difference in the mean Fe–S* bond distance between the two faces is only 0.01 Å [12]. On the other hand, the bond distances of Fe(1) and the terminal sulfur S(1A) (2.270(4) Å), and of Fe(2) and S(1B) (2.273(3) Å) are longer than those of Fe(3) and S(1C) (2.266(3) Å) and of Fe(4) and S(1D) (2.259(3) Å). Such differences are not observed in the crystal structure of $[Fe_4S_4(S\text{-}t\text{-}Bu)_4]^{2-}$. Although a slight conical distortion of the Fe_4S_4 core is observed in $[Fe_4S_4(SAd)_4]^{2-}$ compared with other Fe_4S_4 clusters reported so far, $[Fe_4S_4(SAd)_4]^{2-}$ seemingly has enough space for coordination of H_2O to the Fe_4S_4 core.

Stability of $[Fe_4S_4]^{3+}$ core in aqueous conditions

On the basis of the molecular structure of $[Fe_4S_4(SAd)_4]^{2-}$ and an extreme lability of $[Fe_4S_4(SAd)_4]^-$ in H_2O/DMF (3 vol.%), the size of the SAd^- ligand may not be enough to prevent the coordination of H_2O to the $[Fe_4S_4]^{3+}$ core. The effective enhancement of the stability of $[Fe_4S_4(SAd)_4]^-$ by the presence of free AdSH in H_2O/DMF (23 vol.%) strongly indicates that the hydrolysis of $[Fe_4S_4(SAd)_4]^-$ results from dissociation of the terminal ligand by coordination of H_2O to the $[Fe_4S_4]^{3+}$ core. The distinct difference in the stability of $[Fe_4S_4(SAd)_4]^-$ in the absence of free AdSH between aqueous PDAH and H_2O/DMF solutions, therefore, may be associated with the solubility of AdS^- (or AdSH) in both media. Taking into account the extremely low solubility of AdSH (or AdS^-) in aqueous solution, dissociation of AdS^- from the $[Fe_4S_4]^{3+}$ core may be very difficult in aqueous PDAH solution compared with that in H_2O/DMF. Furthermore, even if such a dissociation of AdS^- occurs in the former, the dissociated AdSH will not be able to leave the micelle in which the cluster is covered. This effect also stabilizes $[Fe_4S_4(SAd)_4]^-$ within the micelle. In accord with this, $(Et_4N)_2[Fe_4S_4(SAd)_4]$ underwent a hydrolysis reaction in H_2O/DMF (10 vol.%) to precipitate a black solid out of the solution in 2 h under N_2, while such a decomposition was not observed in an aqueous PDAH solution at PH 7 in 4 h. We, therefore, propose that the $[Fe_4S_4]^{3+}$ oxidation state of the synthetic Fe_4S_4 cluster as the Hp_{ox} model can be stabilized even in H_2O by depression of dissociation of terminal thiolate ligands from the $[Fe_4S_4]^{3+}$ core.

The present study also reveals that a reversible protonation takes place not only on $[Fe_4S_4(SAd)_4]^{3-}$ and $[Fe_4S_4(SAd)_4]^{2-}$ but also on $[Fe_4S_4(SAd)_4]^-$ in aqueous PDAH solutions similar to that of $[Fe_4S_4(SR)_4]^{2-}$ and $[Fe_4S_4(SR)_4]^{3-}$ (R = aryl or alkyl) in aqueous micellar solutions [15]. Based on an analogy to hydrogen bonding [5] between polypeptide NH protons and core and/or terminal sulfurs(s) of 4Fe Fd and Hp [16], the most reasonable protonation sites of $[Fe_4S_4(SAd)_4]^{n-}$ ($n = 1, 2, 3$) may be core and/or terminal sulfur(s). This result also suggests that the Fe_4S_4 core

of the present cluster is more or less in contact with the aqueous phase even in the presence of PDAH. Thus, $[Fe_4S_4(SAd)_4]^{n-}$ ($n=1$, 2, 3) is not considered to be protected by hydrophobic spheres formed by PDAH.

Although this conclusion is not in accord with the view that the $[Fe_4S_4]^{3+}$ center of Hp_{ox} is protected by hydrophobic spheres formed by polypeptide chains around the Fe_4S_4 core, midpoint potentials of some Hp proteins in a Reiske center are also shifted by -0.06 V/pH [17], as observed in the present study.

Supplementary material

Thermal parameters for non-hydrogen atoms, observed and calculated structure factors and a full list of bond distances and angles are available on request from author K.T.

References

1 C.D. Stout, in T.G. Spiro (ed.), *Iron-Sulfur Proteins,* Vol. 4, Wiley, New York, 1982, Ch. 3.
2 C.W. Carter, Jr., in W. Lovenberg (ed.), *Iron-Sulfur Proteins,* Vol. 3, Academic Press, New York, 1977, Ch. 6.
3 J.M. Berg and R.H. Holm, in T.G. Spiro (ed.), *Iron-Sulfur Proteins,* Vol. 4, Wiley, New York, 1982, Ch. 1.
4 R.H. Holm and J.A. Ibers, in W. Lovenberg (ed.), *Iron-Sulfur Proteins,* Vol. 3, Academic Press, New York, 1977, Ch. 1.
5 R.H. Holm, S. Ciurli and J.A. Weigel, in S.J. Lippard (ed.), *Progress in Inorganic Chemistry,* Vol. 38, Wiley, New York, 1990, Ch. 1.
6 C.W. Carter Jr., J. Kraut, S.T. Freer and R.A. Alden, *J. Biol. Chem., 249* (1974) 6339.
7 H.L. Blonk, O. Kievt, E.-H. Roth, J. Jordanov, J.G.M. van der Linden and J.J. Steggerda, *Inorg. Chem., 30* (1991) 3231.
8 P.K. Mascharak, K.S. Hagen, J.T. Spence and R.H. Holm, *Inorg. Chim. Acta, 80* (1983) 157.
9 N. Ueyama, T. Terakawa, T. Sugawara, M. Fuji and A. Nakamura, *Chem. Lett.,* (1984) 1287.
10 T. O'Sallivan and M.M. Millar, *J. Am. Chem. Soc., 107* (1985) 4097.
11 Y. Okumo , K. Uoto, O. Yonemitsu and T. Tomohiro, *J. Chem. Soc., Chem. Commun.,* (1987) 1018.
12 M. Nakamoto, K. Tanaka and T. Tanaka, *J. Chem. Soc., Chem. Commun.,* (1988) 1422; H. Kambayashi, M. Nakamoto, S.-M. Peng, H. Nagao and K. Tanaka, *Chem. Lett.,* (1992) 919.
13 D. Lexa, J.M. Savene and J. Zickler, *J. Am. Chem. Soc., 99* (1977) 786.
14 C.L. Hill, J. Renaud, R.H. Holm and L.E. Mortenson, *J. Am. Chem. Soc., 99* (1977) 2549.
15 M. Nakamoto, K. Tanaka and T. Tanaka, *Bull. Chem. Soc. Jpn., 61* (1988) 4099; K. Tanaka, M. Moriya and T. Tanaka, *Inorg. Chem., 25* (1986) 835.
16 G. Backes, Y. Mino, T.M. Loehr, T.E. Meyer, M.A. Cusanovich, W.V. Sweeney, E.T. Adman and J. Sanders-Loehr, *J. Am. Chem. Soc., 113* (1991) 2055.
17 R.C. Prince and P.L. Datton, *FEBS Lett., 65* (1976) 117.